Analyst

Volume 1 | Number 1 | Jan 2013 | Pages 1–100

Analyst

www.rsc.org/analyst

ROYAL SOCIETY OF CHEMISTRY

www.rsc.org/analyst

Analyst

PAPER

Robust Electrochemiluminescence Immunoassay for Carcinoembryonic Antigen Detection based on Microtiter Plate as Bridge and Au@Pd Nanorods as Peroxidase Mimic

Yong Zhang,[a,b] Xuehui Pang,[b] Dan Wu,[c] Hongmin Ma,[c] Zhaoqing Yan,[b] Jiatao Zhang,[*a] Bin Du[*c] and Qin Wei[*b]

The common drawbacks of most traditional electrochemiluminescence (ECL) immunoassays are the strict storage conditions of ECL electrode and the steric hindrance caused by bovine serum albumin and antigen. The strict storage conditions require the modified electrode must be stored at 4 °C before measurement, which may cause the degradation of protein molecules and low reproducibility as the time goes by. The steric hindrance can hinder the electron transfer between the electrode and the electrochemical active substance unable to transmit proteins on the electrode surface. The current study takes 96-well microtiter plate (MTP) as bridge for analyte pre-treatment and Au@Pd nanorods as peroxidase mimic to assemble a simple and robust ECL immunoassay. Advantages of such assay include not only high sensitivity but also robust detection circumstance. We demonstrated the method by detecting carcinoembryonic antigen from human serum and got a good detection limit of 3 fg·mL⁻¹.

Introduction

Electrochemiluminescence (ECL) as a useful analytical technique has been established in the past decade, and is still gaining momentum.[1-3] In ECL assays, the chemiluminescent reaction is electrically initiated. The reactive species which can react with one another to produce light are generated from stable precursors (i.e., the ECL-active label) at the surface of an electrode. Besides it can be precisely controlled, ECL technology has many distinct advantages over other detection methods, such as simple fabrication and high sensitivity with low background.[4-7] Therefore, ECL immunoassay exhibits great potential in biomedical applications. In general, three types of ECL immunoassays, including label-free, sandwich-type and competitive assays, have been developed to date. The principle of label-free ECL immunoassay is that the luminescent signal can be decreased by the steric hindrance produced from the antibody-antigen (Ab-Ag) immune-complexation. In the other two types, the ECL signals can be altered by the enzymatic signal generated reaction.[8-13] However, one of their common drawbacks is that antibodies

immobilization on the electrodes can increase the steric hindrance, which can hinder the electron transfer between the electrode and the electrochemical active substance.[14-16] The main reason to hinder the electron transfer by the steric hindrance is most of the protein macromolecules are not conductive. Therefore, the density of the antibodies on the surface cannot be too high to minimize steric hindrance.[17] In addition, the other common drawback of all such assays is that the modified electrodes have to be stored at 4 °C before measurement. Otherwise, low reproducibility may be caused as the time goes by, due to the degradation of protein molecules. These two drawbacks limit their applications and development.

Compared with horse radish peroxidase (HRP), peroxidase mimic has robust and stable merits. Specially, noble metal nanoparticles (NPs) as peroxidase mimic received widespread attention[18]. Due to the advantages, including easy preparation, high homogeneity, and biocompatibility with proteins, Au NPs have been regarded as a versatile template for the immobilization of biomolecules and also play an important role in numerous fields of biomedical applications.[19-21] In addition, Pd and Ag NPs with superior electrochemical properties can facilitate the electron transfer from the redox center of protein to the electrode surface. So bimetallic NPs such as Au/Ag and Au/Pd also attracted widespread attention especially in the field of immunoassay, and they often showed better electrochemical performance than their monometallic counterparts.[22]

Cancer biomarkers, which are some kind of proteins expressed with high abundance in blood under abnormal physiological conditions, can be used for early diagnosis of

a. School of Materials Science & Engineering, Beijing Institute of Technology, Beijing 100081, PR China. E-mail: zhangjt@bit.edu.cn; Fax: +86-10-68918065; Tel: +86-10-68918065.
b. School of Chemistry and Chemical Engineering, University of Jinan, Jinan 250022, PR China. E-mail: sdjndxwq@163.com; Fax: +86-531-82765969; Tel: +86-531-82765730.
c. Key Laboratory of Chemical Sensing and Analysis in Universities of Shandong, Jinan 250022, PR China. E-mail: dubin61@gmail.com; Fax: +86-531-82767370; Tel: +86-531-82767370.
†Electronic Supplementary Information (ESI) available. See DOI: 10.1039/x0xx00000x

diseases.[23,24] To rapidly detect such biomarkers for point-of-care of cancer diagnostics, simple immunoassays are desirable. Colorimetric immunoassay is a developed method for biomarker detection. Probably due to the vulnerable/limited signal amplification strategies applied, the sensitivity of colorimetric immunoassay is not always satisfying.[25] Therefore, successful detection of cancer biomarkers, which are usually present with very low concentration, is not easily achievable. Nevertheless, because it can realize high-throughput detection by means of microtiter plate (MTP), colorimetric immunoassay is potential to be applied for clinical detection.[26]

In this study, we present a novel design of using 96-well MTP as bridge and Au@Pd nanorods (NRs) as peroxidase mimic for biomarker detection. After bio-samples are treated in 96-well MTP to get high throughput under biological environment, they are detected by ECL assay to get high sensitivity under robust environment. As a proof-of-principle, carcinoembryonic antigen (CEA) was analysed from human serum, and achieved higher sensitivity, higher throughput and better sensitivity compared with conventional ECL immunoassay.

Experimental

Materials and reagents

All chemicals were used as-received without further processing. Luminol was purchased from TCI Co. Ltd. (Hong Kong, China). K_2PdCl_4, $HAuCl_4 \cdot 4H_2O$ and $AgNO_3$ were obtained from Shanghai Chemical Reagent Co., Ltd. (Shanghai, China).

Cetyltrimethylammonium bromide (CTAB), ascorbic acid (AA), glutaraldehyde (GA) and graphite powder were provided by Shanghai Sinopharm Chemical Reagent Co., Ltd (Shanghai, China). 3,3′,5,5′-tetramethylbenzidine (TMB) and Nafion (5%) were obtained from Sigma-Aldrich (Beijing, China). Bovine serum albumin (BSA, 96-99%) was purchased from Sigma (USA) and used as received. CEA and CEA antibody (anti-CEA) were purchased from Wanger Biotechnology Co., Ltd. (Beijing, China). All other reagents were of analytical grade. Phosphate buffered saline (PBS, 0.1 mol·L^{-1} containing 0.1 mol·L^{-1} NaCl) was used as electrolyte for all electrochemistry measurements. High-binding polystyrene 96-well MTP was obtained from Greiner Bio-One (Frickenhausen, Germany, cat#: 655061). Deionised water was prepared by a Millipore Milli-Q system and used throughout.

Apparatus

Double-step potential (DSP) experiments were performed on CHI 760D electrochemical workstation (Shanghai, China). The ECL intensity was measured with MPI-ECL Analyzer (Xi'an Remax Electronic High-Tech Ltd) with the voltage of the photomultiplier tube set at 800 V in the process of detection. Electrochemical impedance spectroscopy (EIS) was obtained from the impedance measurement unit (IM6e, ZAHNER elektrik, Germany). All electrochemical and ECL experiments were carried out in a conventional three-electrode cell with a modified glassy carbon electrode (GCE, diameter 4 mm) as the working electrode, a Pt wire electrode as the counter electrode and an Ag/AgCl electrode as the reference electrode.

The UV-Vis absorption spectra of water colloid were recorded by a plate reader (DNM-9602, Beijing Perlong Medical Instrument Ltd, China). The absorbance of TMB-H_2O_2 reaction on MTP was read at 650 nm with a plate reader (DNM-9602, Beijing Perlong Medical Instrument Ltd, China). TEM (JEOL JEM 1200EX working at 100 kV) and high-resolution TEM (HRTEM, FEI Tecnai G2 F20 S-Twin working at 200 kV) were utilized to characterize morphology and interfacial lattice details.

Preparation of Au NRs and Au@Pd NRs

Au NRs were synthesized via a typical seed mediated growth method with some modifications.[27] Briefly, Au-seeds aqueous solution was firstly prepared by adding 0.6mL of ice-cold 10 mmol·L^{-1} $NaBH_4$ to 10 mL of solution containing 0.10 mol·L^{-1} CTAB and 0.25 mmol·L^{-1} $HAuCl_4$. After vigorous stirring for 30 s, the resulted brownish yellow solution was undisturbed at 25 °C for 30 min. Then, the growth solution was prepared via successively adding 0.35 g KBr, 1.2 mL of 4 mmol·L^{-1} $AgNO_3$, 25 mL of 1 mmol·L^{-1} $HAuCl_4$ and 0.45 mL of 64 mmol·L^{-1} AA to 0.10 mol·L^{-1} CTAB aqueous with stirring in the whole procedure. At last, 0.08 mL Au-Seeds was added to the growth solution and undisturbed at 25 °C for 12 h. After the color changed from colorless to dark blue, Au NRs were obtained and centrifugated twice at 6000 rpm for 10 min. Finally, Au NRs were dispersed in 4 mL of CTAB (0.1 mol·L^{-1}).

For preparing Au@Pd NRs, the obtained Au NRs were used as seed for the followed preparation of Au@Pd NRs, which can be simply prepared via the following steps: 300 μL of 0.1 mol·L^{-1} AA, 50 μL of 10 mmol·L^{-1} K_2PdCl_4, and 300 μL of 0.1 mol·L^{-1} NaOH were successively added to 5 mL Au NRs solutions under stirring at 25 °C. After 30 min, the Au@Pd NRs solution was centrifuged (6000 rpm for 15min) followed by consecutive washing three times with deionised water and the resulted precipitates were re-dispersed in 2 mL of PBS (pH 7.4) for the later reaction. This pathway produced Au@Pd NRs with an aspect ratio of ~ 3.6 and an average length of 30 nm.

Preparation of Au@Pd/luminol-Ab$_2$

A luminol stock solution (0.01 mol·L^{-1}) was prepared firstly by dissolving luminol in 0.1 mol·L^{-1} NaOH. Au@Pd NRs and luminol labeled secondary anti-CEA (Au@Pd/luminol-Ab$_2$) were synthesized via incubation with 0.5 mL of luminol stock solution and 0.5 mL of anti-CEA (10 μg·mL^{-1}) and the mixture was shaken overnight on table concentrator in dark place. Following purified by centrifugation, the product was re-dispersed into 2 mL of PBS (pH 7.4). Then 250 μL of 1% BSA solution was added and incubated at room temperature for 0.5 h to block nonspecific binding and avoid the nonspecific adsorption on Au@Pd NRs. After continued purified by centrifugation and re-dispersed into 2 mL of PBS (pH 7.4), Au@Pd/luminol-Ab$_2$ was obtained and stored in a dark place at 4 °C.

Preparation of NH$_2$-graphene (NH$_2$-G)

Firstly, the graphite oxide (GO) powders were synthesized according to the reported method with some improvements.[28] In the typical preparation, the mixture of graphite powder (0.3 g) and $KMnO_4$ (1.8 g) was added into the mixture solution of H_2SO_4 and H_3PO_4 at a molar ratio of 9:1. After the reaction mixture was heated to 50 °C with constant stirring for 12 h, the

mixture solution was poured onto ice (40 mL) containing 0.3 mL of H_2O_2 (30 %). The product was collected by centrifugation at 9000 rpm for 10 min. The remaining precipitate was washed
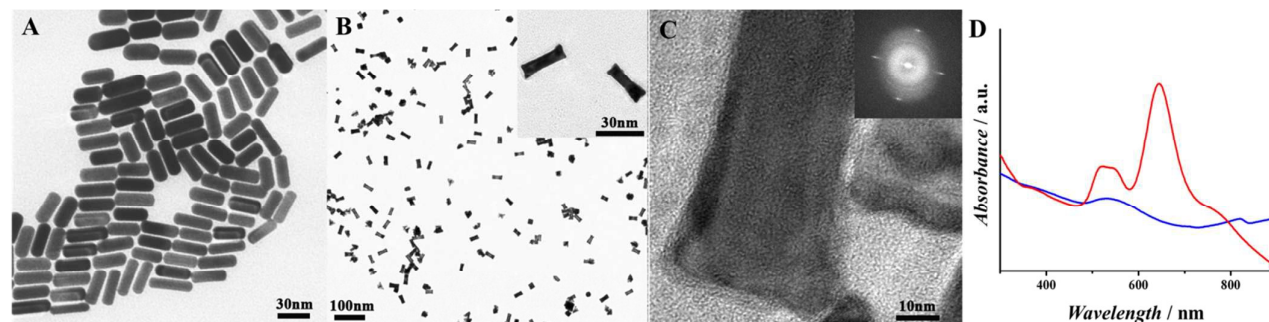

Fig. 1 (A) TEM image of Au NRs. (B) TEM image of Au@Pd NRs, Local Zoom (inset). (C) HRTEM image of Au@Pd NRs, the FFT pattern (inset). (D) UV/Vis absorbance of Au NRs (red) and Au@Pd NRs (blue).

two times with HCl (0.2 mol·L^{-1}), ethyl alcohol and diethyl ether, respectively. Finally, the GO powders were obtained after the product was dried in vacuum at 35 °C and grinded in a quartz mortar.

Secondly, 200 mg of GO powder was added to ethylene glycol (80 mL) under ultra-sonication for 30 min, followed by the addition of 2 mL of $NH_3·H_2O$ under constant stirring for several minutes. Then, the dark brown solution was transferred into autoclave for solvothermal reaction at 180 °C for 10 h. The obtained NH_2-G precipitation was washed three times with deionised water, and dried in vacuum at 50 °C.[29]

Pre-treatment procedure of the measurements

First, per well of MTP was coated with 50 μL of anti-CEA (Ab_1, 100 μg·mL^{-1}) in PBS buffer (pH 7.4) for 12 h at 4 °C according to the previous report.[26] Then, 200 μL of 1 % BSA solution as blocking buffer per well was used to suppress the nonspecific adsorption to the plates for 2 h at 4 °C. At the end of every step above were all along with a washing step of using PBS buffer (pH 7.4). Before the ECL or colorimetric measurements were operated, 50μL of different concentration of CEA standards or real samples were added and incubated for 2 h at 4 °C. Lastly, after washed by PBS (pH7.4), 50 μL of Au@Pd/luminol-Ab_2 were added and incubated for 2 h at 4 °C.

Fabrication and measurement of ECL immunoassay

Before use, GCE was polished using a polishing cloth (CHI Inc.) with small particles (1.0 and 0.05 mm) of Al_2O_3 slurry, rinsed with water, and then ultrasonic in ethanol and ultra-pure water. Then 10 μL of 2 mg·mL^{-1} NH_2-G was added onto the GCE surface. After dried, 5 μL of Nafion (5 %) was added to form a matrix film in order to prevent NH_2-G falling off from the electrode surface. Finally, 3 μL of GA solution (2.5 %, v/v) was added onto the matrix film for better antibody adsorption.

After being washed, the prepared GCE was ready for the later experiment.

ECL measurement was operated as following description: after the MTP was pre-treated according to the above pre-treatment procedure, 10 μL of Au@Pd/luminol-Ab_2 was pipetted from the upper solution in the well and modified onto the prepared GCE. With no necessary consideration of biological environment, the modified GCE was dried and used as the working electrode. ECL measurement was performed in an ECL cell containing 10 mL of 0.1 mol·L^{-1} PBS (pH 7.4) solution with 1.5 mmol·L^{-1} H_2O_2. The generation of ECL response resulted from electrochemical reactions of luminol on the surface of the Au@Pd/luminol-Ab_2 in the presence of H_2O_2. ECL signals were generated and recorded using DSP with the parameter: initial potential 0 V, pulse potential 0.9 V, pulse period 30 s and pulse time 0.1 s.[12]

Measurement of colorimetric assay

Colorimetric measurement was operated as following description: after the MTP was pre-treated according to the above pre-treatment procedure, the upper solution of the unbound Au@Pd/luminol-Ab_2 in the well was washed using PBS buffer (pH 7.4). Then, 100 μL of substrate solution containing 1 mol·L^{-1} H_2O_2 and 4 mmol·L^{-1} TMB in pH 3.2 sodium acetate buffer solution was added and incubated at 37 °C for 10 min, the absorbance was read at 652 nm for catalysis comparison. For calibration curve detection, after 10 min for color development, the catalytic reaction was stopped by adding 50 μL of 2 mol·L^{-1} H_2SO_4 to each well and the absorbance of color products were recorded at 452 nm.

Results and discussion

Materials characterization

To better understand the size distribution of Au@Pd NRs, transmission electron microscopy (TEM) and high-resolution TEM (HRTEM) were used for characterization (Fig. 1). Au NRs with an aspect ratio of ~3.2 and an average length of 30 nm were firstly synthesized and well dispersed (Fig. 1A). After coating Pd NPs, bone-like Au@Pd NRs with single-crystal structure (Fig. 1B and 1C) were formed, based on the preferentially adopting epitaxial growth of Pd on Au surface.[30]

In this work, Au@Pd NRs with 30 nm (Fig. 1B) were chosen because this was a balanced and appropriate size for combining antibodies, which could be explained by Rubik's cube theory.[31] In brief, because the antibody is about 10-15 nm, if Au@Pd NRs are smaller than the size of antibody (the loading substrate and antibody are not in a comparative size), the antibodies
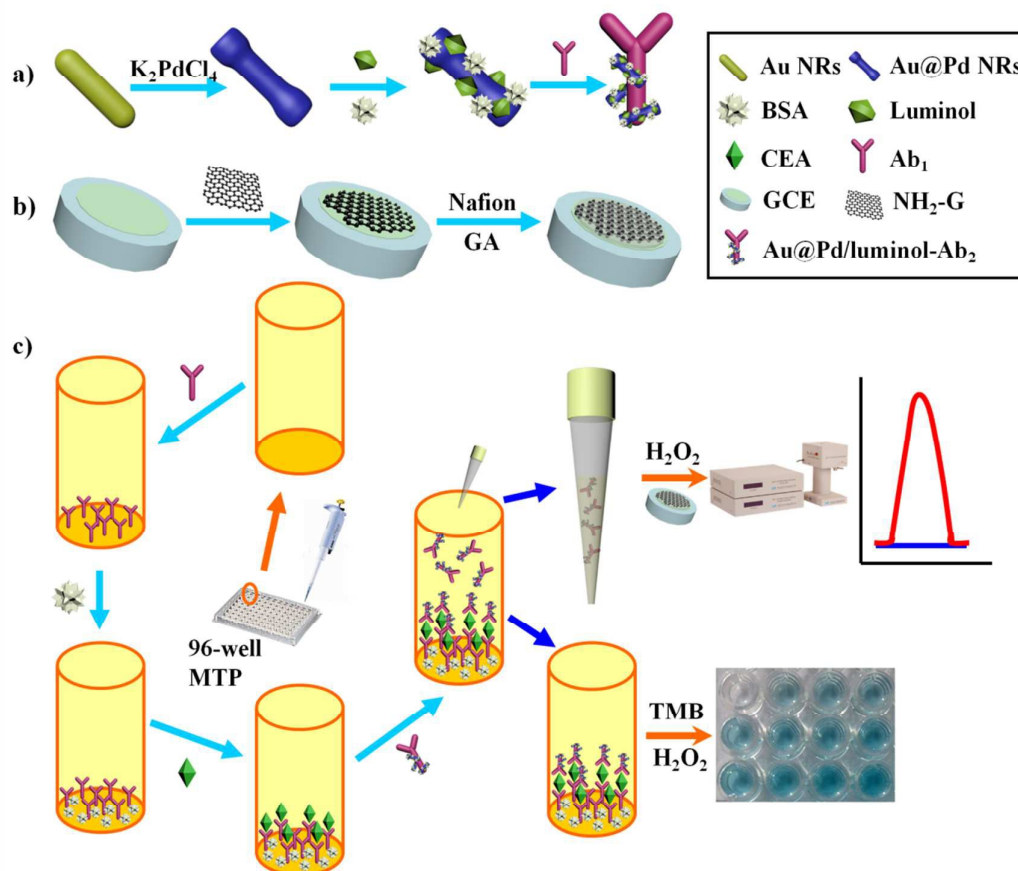
Scheme 1 Schematic illustration of the fabrication and detection procedures of ECL immunoassay by means of 96-well MTP: (a) Preparation of Au@Pd NRs and Au@Pd/luminol-Ab$_2$. (b) Preparation of NH2-G. (c) Fabrication and measurement of ECL immunoassay and colorimetric assay.

cannot be combined well on the substrate due to the limitation of size. In another aspect, if Au@Pd NRs are much larger, for example, over a hundred nanometers, the substrate is many times larger than antibody in size which may leave over many nonspecific active sites resulting in the inaccuracy of the results. Corresponding UV-vis extinction spectra of the Au NRs (red line) and Au@Pd NRs (blue line) were illustrated in Fig. 1D. Au NRs showed a longitudinal surface plasma resonance (SPR) peak at 682 nm and a transverse SPR band centred at 510 nm. After Pd shell was coated, the SPR peak of Au NRs was gradually damped suggesting Pd atoms were grown on Au NRs surface. This is because the conductivity of Pd atoms at optical frequency is much lower than that of Au

atoms.[30] NH$_2$-G was synthesized according to our previous work[29] and well dispersed in solution (see Fig. S1†).

Immunoassay fabrication characterization

Scheme 1 illustrates the overview of the fabrication and measurement of the immunoassay. First, Au@Pd NRs and luminol coefficient labelled anti-CEA were synthesized (scheme 1a). In the meantime, NH$_2$-G was prepared and modified onto GCE (scheme 1b) for later use. Then, as shown in scheme 1c, a high-binding polystyrene 96-well MTP was coated with Ab$_1$. After blocking the active sites with BSA, solutions containing CEA standards or real samples with various concentrations were added into the MTP wells. Following that, 50μL of

Au@Pd/luminol-Ab$_2$ with the same concentrations was added. After Ab-Ag immunoreactions, 10 μL unbound Au@Pd/luminol-Ab$_2$ from the upper solution in the well was measured by pipetting onto the GCE prepared previously. Following quick dry at room temperature, the modified GCE was measured by ECL assay via luminol-H$_2$O$_2$ system. The ECL signal corresponding to the concentration of unbound Au@Pd/luminol-Ab$_2$ is inversely proportional to the concentration of CEA. For proving the sum of combined and unbound Au@Pd/luminol-Ab$_2$ was consistent, after unbound

Au@Pd/luminol-Ab$_2$ was washed off the wells, 100 μL of substrate solution containing TMB and H$_2$O$_2$ was added. Because of the catalytic effect of Au@Pd NRs to colorimetric system of TMB-H$_2$O$_2$, different colors in the wells containing various concentrations of Au@Pd/luminol-Ab$_2$ binded to the bottom of well were visualized. The corresponding absorbance intensity is in direct proportion to the concentration of CEA.
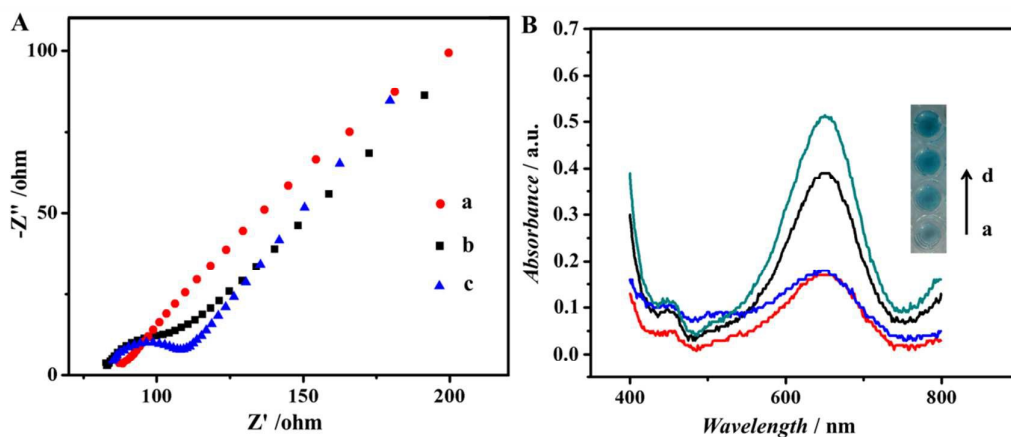

Fig. 2 (A) Nyquist plots of the EIS for immobilized step recorded from 0.1 to 10^5 Hz of (a) bare GCE, (b) NH$_2$-G/GA/nafion/GCE, (c) Au@Pd/luminol-Ab$_2$/GA/nafion /NH$_2$-G/GCE in 1 mmol·mL^{-1} Fe(CN)$_6^{3-/4-}$ solution. (B) A comparison of colorimetric assay after H$_2$O$_2$ and TMB were added and 10 min for color development: (a) Ab$_1$-CEA, (b) Ab$_1$-CEA/luminol, (c) Ab$_1$-CEA-Au/luminol-Ab$_2$, (d) Ab$_1$-CEA-Au@Pd/luminol-Ab$_2$.

The assembly process of the modified GCE used in ECL assay was also characterized by EIS. EIS is an effective method to monitor the assembly of the immunoassay and probe the feature of the modified electrode surface.[32] The EIS profile of bare GCE was almost a straight line (curve a in Fig. 2A), characteristic of the diffusion limiting step of the electrochemical process. Because its advantages of good conductivity and high surface areas, NH$_2$-G was used as substrate modified on GCE for ECL detection. As expected, when the NH$_2$-G uniting matrix with nafion and GA modified electrode, the EIS was similar to that of the bare GCE (curve b in Fig. 2A). One of the possible reasons is the matrix immobilized on the electrode is similar to a conducting wire, which makes it easier for the electron transfer.[33] The electron transfer resistance increased dramatically after Au@Pd/luminol-Ab$_2$ (curve c in Fig. 2A) was dropped on the modified GCE and increased successively with the increase of Au@Pd/luminol-Ab$_2$ concentration. This is because of the steric hindrance effect by the non-conductive biological molecules.[34] It is also can be as the evidence of good adsorption of Au@Pd/luminol-Ab$_2$ on the modified GCE.

Mechanism and analytical performance of the ECL immunoassay

To better demonstrate Au@Pd NRs as peroxidase mimic played an essential role in our strategy, the peroxidase-like catalytic activity of Au@Pd/luminol-Ab$_2$ was studied in the

catalysis of TMB oxidation with H$_2$O$_2$, respectively. When Au@Pd/luminol-Ab$_2$ was added (curve d in Fig. 2B), the absorbance intensity was greatly increased after 10 min at 652 nm, characteristic peak of oxidized TMB. Comparing to the minimal change of absorbance intensity of Ab$_1$ and CEA immobilized in the MTP wells (curve a in Fig. 2B), Au@Pd/luminol-Ab$_2$ showed an intrinsic peroxidase-like activity. To exclude the possible catalytic activity of luminol, the luminol for catalytic TMB-H$_2$O$_2$ reaction was put alone, and no obvious catalytic reaction was observed in this system (curve b in Fig. 2B) as expected, indicating that Au@Pd NRs played the peroxidase mimic role and were crucial for the formation of Au@Pd/luminol-Ab$_2$. In addition, the catalytic of Au NRs was compared with Au@Pd NRs. Although under the same conditions Au NRs can catalyse TMB-H$_2$O$_2$ reaction (curve c in Fig. 2B), the absorbance of Au NRs catalytic system has obviously lower intensity than Au@Pd NRs catalytic system at 652 nm, probably due to the fact that the catalytic activity of Pd is higher than Au.[35]

To further prove feasibility of the ECL immunoassay, ECL signals were investigated before and after Au@Pd/luminol-Ab$_2$ modified the prepared GCE. No ECL signal can be seen when the GCE was modified with NH$_2$-G only (curve a in Fig. S2†), whereas strong ECL signal was observed when the Au@Pd/luminol-Ab$_2$ was introduced to the prepared GCE via the stable cross-linked action of GA to amine groups between

NH$_2$-G and antibody (curve b in Fig. S2†). The dramatic increase of ECL signal is due to the emission of luminol-H$_2$O$_2$ ECL system catalysed by Au@Pd NRs. The Au@Pd NRs is concentrated close to the electrode surface, so they can be shaped and accurately positioned for optical measurement system with maximum sensitivity.[3] This phenomenon also indicated that As illustrated in Fig. 3A, the ECL intensity decreased gradually while increasing antigen concentrations. Taking into account of the direct electron transfer and electrogenerated chemiluminescence without the steric hindrance produced by other proteins (i.e. BSA and antigen) on the electrode surface, our immunoassay achieved a promising

analytical performance. The standard calibration curve of CEA detection is shown in inset of Figure 3A suggested that the ECL intensity decreased linearly in the range of 0.01 pg·mL^{-1} to 100 ng·mL^{-1} CEA. The linear equation is $I = 5893 - 894\ \lg C_{CEA}$ (unit of C_{CEA} is ng·mL^{-1}) with a correlation coefficient of 0.9934. The detection limit is 3 fg·mL^{-1}. According to the linear equation, trace amount of CEA concentration quantitatively detected by our ECL immunoassay, which is comparable to other published methods[36-39] as shown in Table 1. Our detection
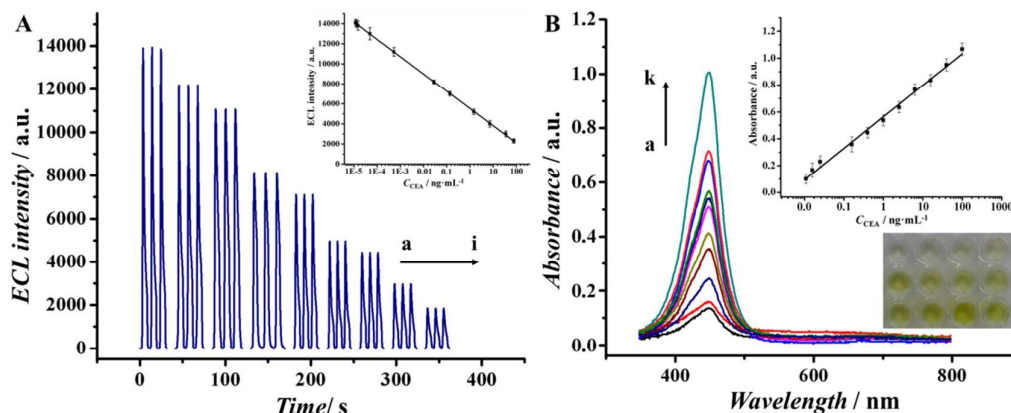

Fig. 3 (A) ECL response for different concentrations of CEA: 0, 1E-5, 1E-4, 1E-3, 0.01, 0.1, 1, 10, 100 ng·mL^{-1} (curve a to i). (B) Absorbance for different concentrations of CEA: 0.01, 0.05, 0.1, 0.5, 1, 5, 10, 25, 50, 75, 100 ng·mL^{-1} (curve a to k) after 10 min for color developing, visual detection (inset). Insets of (A) and (B) are calibration curves of the immunoassay for different concentrations of CEA.

limit decreased two or more orders of magnitude.

Analytical performance of the colorimetric assay

The colorimetric assay in our work can be used to further confirm feasibility of our strategy. Because the unbound Au@Pd/luminol-Ab$_2$ from the upper solution in the well can be sensitively detected by ECL assay and the concentration of Au@Pd/luminol-Ab$_2$ is inverse proportion to the concentration of CEA, the combined Au@Pd/luminol-Ab$_2$ in the well via Ab-Ag immunoreactions should be in direct proportion to CEA. Therefore, after washing away the unbound Au@Pd/luminol-Ab$_2$ from the MTP wells, the bound Au@Pd/luminol-Ab$_2$ can be used as signal detection probes to catalyse the TMB oxidation and produce colorimetric signals. Following the same procedure as the conventional ELISA, H$_2$SO$_4$ was used to stop the catalytic reaction where the oxidized TMB was further oxidized to a yellow diimine with the maximum absorption wavelength of 452 nm. So the absorbance intensity in the UV-vis spectra at 452 nm was recorded to quantify the CEA. It can be observed in Fig. 3B that the absorbance at 452 nm increased while CEA concentration increased. Meanwhile, there was a visually observable color change correlated to CEA concentrations. Inset of Fig. 3B showed the absorption intensity was linear to the concentrations of CEA in the linear

range from 0.01 ng·mL^{-1} to 100 ng·mL^{-1} with a detection limit of 3 pg·mL^{-1}. Comparing with ECL assay in our work, colorimetric assay has a narrower linear range and higher detection limit. One possible reason is that the conjugation of Au@Pd NRs with protein molecules caused the decrease the decrease of Au@Pd NRs catalytic efficiency.

Detection conditions optimization

The above described optimal conditions were investigated and illustrated in Fig 4 A-E. Firstly, pH values of both ECL assay and colorimetric assay were optimized (Fig. 4A). When the pH values of measurement solution were 7.4 for ECL assay and 9.2 for colorimetric assay, these two assays displayed the optimal signal intensity. Then, the concentration of NH$_2$-G in our study is an important factor that would affect the performance of ECL assay, because it is used as substrate for Au@Pd/luminol-Ab$_2$ loading. As shown in Fig. 4B, when concentrations of NH$_2$-G changed from 1.0 to 2.0 mg·mL^{-1}, the ECL intensity increased gradually and reached the maximum at 2.0 mg·mL^{-1}. However, with further increasing concentrations of NH$_2$-G from 2.0 to 3.0 mg·mL^{-1}, the ECL intensity decreased slightly. One of the possible reasons is that excessive NH$_2$-G may be stacked each other.[27] Therefore, 2 mg·mL^{-1} was chosen as the best concentration of NH$_2$-G for subsequent experiments. To get

the optimal concentration of luminol, luminol solutions with different concentration were used for preparing Au@Pd/luminol-Ab$_2$ and measured by ECL assay. As illustrated in Fig. 4C, when 0.010 mol·L^{-1} luminol was used, ECL intensity achieved the maximum. So 0.010 mol·L^{-1} luminol was chosen as the optimal condition. The effect of developing time for the

Table 1 Comparison of different ECL immunoassays for CEA detection in terms of linear range and detection limit.

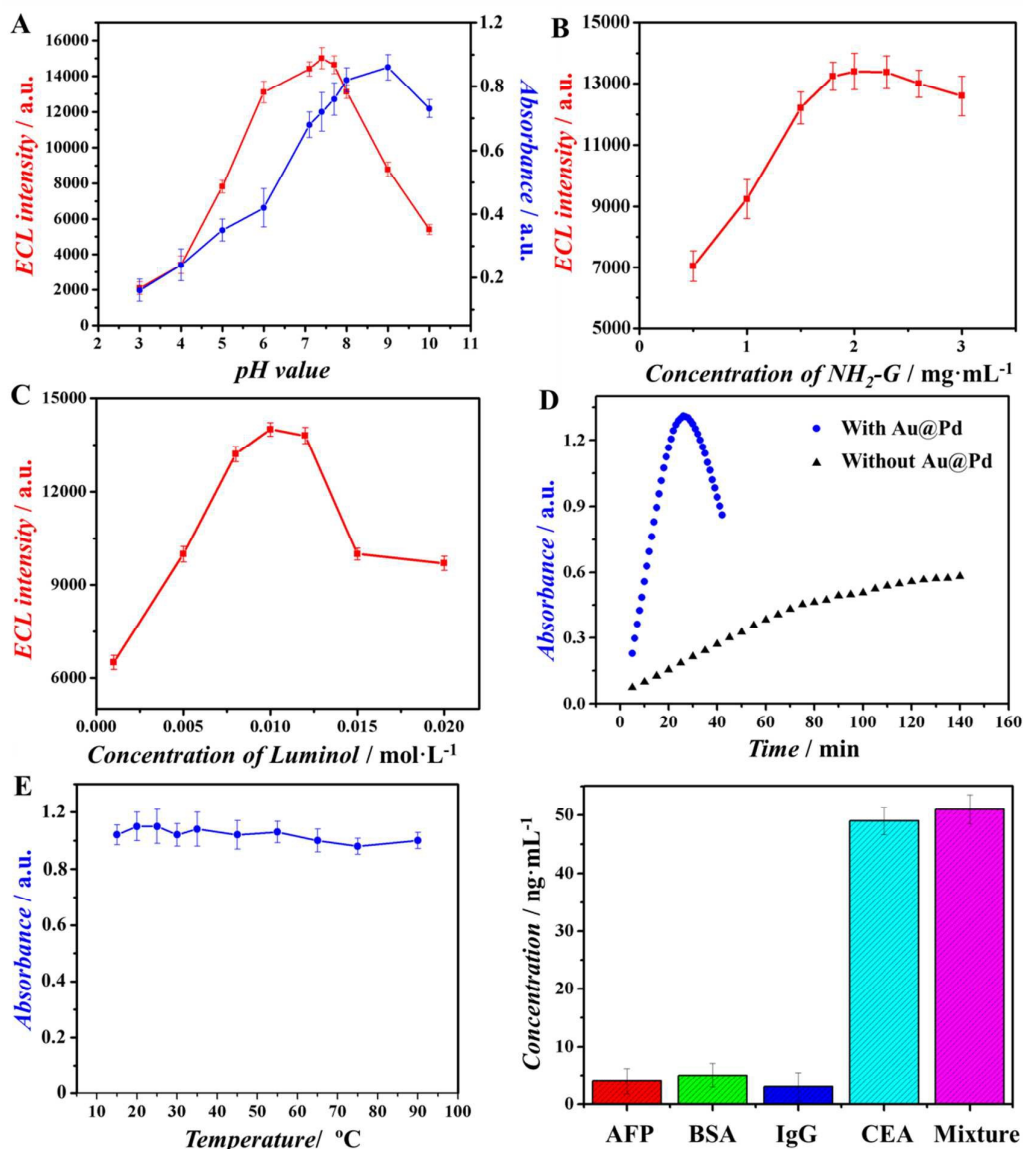| References	Linear range	Detection limit
36	1 pg·mL^{-1} ~ 50 ng·mL^{-1}	0.7 pg·mL^{-1}
37	50 pg·mL^{-1} ~ 200 ng·mL^{-1}	10 pg·mL^{-1}
38	1 pg·mL^{-1} ~ 200 ng·mL^{-1}	0.4 pg·mL^{-1}
39	5 fg·mL^{-1} ~ 50 pg·mL^{-1}	1.52 fg·mL^{-1}
This work	10 fg·mL^{-1} ~ 100 ng·mL^{-1}	3 fg·mL^{-1}

Fig. 4 Optimization of the experimental parameters: (A) pH value on the response of the ECL (red) and colorimetric (blue) assay; (B) the amount of NH$_2$-G on the response of the ECL assay; (C) the amount of luminol on the response of the ECL assay; (D) time of color developing in the colorimetric assay; (E) temperature of color developing in the colorimetric assay. (F) A comparison of

ECL assay for detecting CEA with those of different interfering species: 50 ng·mL^{-1}AFP, 50 ng·mL^{-1} BSA, 50 ng·mL^{-1} IgG, 50 ng·mL^{-1} CEA and mixture (50 ng·mL^{-1} CEA, 50 ng·mL^{-1}AFP, 50 ng·mL^{-1} BSA and 50 ng·mL^{-1} IgG).

operation circumstance in colorimetric assay was optimal as 20 min (Fig. 4D) because of the catalytic property of Au@Pd NRs. Finally, the optimal temperature for operating colorimetric assay was investigated. Au@Pd NRs were used as peroxidase mimic and no consideration of enzyme inactivation was needed, colorimetric assay was almost not influenced by temperature (Fig. 4F).

Specificity, reproducibility and stability of the immunoassay

Since the antibody lifetime is not an issue, our ECL assay demonstrated impressive stability and reproducibility. In this study, after the modified GCE was stored under room temperature for four weeks, the ECL response decreased only ~ 1.5 % of its initial value. Such good stability may attribute to three reasons. The first is that the modified GCE need not consider the biological activity loss of proteins; the second is that Au@Pd NRs as peroxidase mimic has robust and stable merits; the last is the large specific surface area and good

Table 2 Determination of CEA added in human plasma with the ECL immunoassay.

Initial Human plasma (ng·mL^{-1})	The addition content (ng·mL^{-1})	The detection content (ng·mL^{-1})	RSD/%, n=5	recovery/%
0.3	0.1	0.150	3.5	112
0.3	0.5	0.540	3.2	102
0.3	1.0	1.13	3.3	110
3.5	10.0	10.43	2.8	101
12.1	100.0	101.4	2.5	100

electron transfer ability of NH$_2$-G modified on the electrode surface. The relative standard derivation (RSD) of the replicate measurements of CEA at 10 ng·mL^{-1} within a day (intra-day precision, n=5) was 0.5 %; the RSD over 7 days (inter-day precision, n=5) was 1.2 %, which showed good reproducibility.[40]

To characterize the specificity of the immunoassay, various interfering species, including AFP, BSA and IgG, were used in the MTP wells for immunoreactions via ECL assay. Results indicated that these proteins showed negligible interference to the determination of CEA (Fig. 4F), indicating good selectivity of our immunoassay. This could be explained by the fact that Au@Pd NR is a kind of noble metal nanomaterials, which may prevent the binding affinity loss of biomolecules. Therefore, the immunoassay in this study can be used for the detection of CEA in serum samples.

Application in analysis of samples

To evaluate the feasibility of our immunoassay for clinical diagnosis, the concentration of CEA in human plasma was analysed. The human plasma samples were diluted 10 times with 0.1 mol·L^{-1} PBS buffer (pH 7.4) before analysis. Then, CEA was spiked in with different concentrations (0.1, 0.5, 1.0, 10.0 and 100.0 ng·mL^{-1}), and analysed by ECL assay. Results showed that the recovery was in the range of 100 - 112 % and RSD was in the range of 2.5 - 3.5 % (Table 2). These results indicated that the proposed ECL immunoassay could be suitable to the clinical determination of CEA levels in human plasma.

Conclusions

In summary, we provide a novel strategy for preparing a robust ECL immunoassay by means of MTP and Au@Pd NRs. Due to the good catalytic property of Au@Pd NRs and the

direct electron transfer for ECL without the steric hindrance produced by BSA and antigen compared with traditional ECL immunoassay on the electrode surface, our ECL immunoassay has three advantages over conventional methods for CEA detection: low detection limit, robust conditions for measurement and high-throughput. Importantly, our strategy opened a new window for the applying of nanomaterials in the immunoassay field and can be broadly applied to many other similar technologies, such as electrochemical immunoassay and photoelectrochemical immunoassay, etc.

Acknowledgements

References

1   Y. Dong, T. Gao, Y. Zhou and J. Zhu, *Analytical Chemistry*, 2014, **86**, 11373.
2   A.W. Knight, *TrAC Trends in Analytical Chemistry*, 1999, **18**, 47.
3   X. Yin, S. Dong and E. Wang, *TrAC Trends in Analytical Chemistry*, 2004, **23**, 432.
4   S. Deng, J. Lei, Y. Liu, Y. Huang and H. Ju, *Chemical Communications*, 2013, **49**, 2106.
5   A. Devadoss,, C. Dickinson,, T.E. Keyes and R.J. Forster, *Analytical Chemistry*, 2011, **83**, 2383.
6   X. Jiang, Y. Chai, H. Wang and R. Yuan, *Biosensors and Bioelectronics*, 2014, **54**, 20.

Analyst Accepted Manuscript

7   Y. Zhang, F. Lu, Z. Yan, D. Wu, H. Ma, B. Du and Q. Wei, *Microchim Acta*, 2015, **182**, 1421.

8   H. Dai, Y. Wang, X. Wu, L. Zhang and G. Chen, *Biosensors and Bioelectronics*, 2009, **24**, 1230.

9   Y. Dong, W. Tian, S. Ren, R. Dai, Y. Chi and G. Chen, *ACS Applied Materials & Interfaces*, 2014, **6**, 1646.

10 T. Huang, Q. Meng and G. Jie, Biosensors and Bioelectronics, 2015, **66**, 84.

11 C. Li, J. Lin, Y. Guo and S. Zhang, *Chemical Communications*, 2011, **47**, 4442.

12 D. Tian, C. Duan, W. Wang and H. Cui, *Biosensors and Bioelectronics*, 2010, **25**, 2290.

13 H. Xia, L. Li, Z. Yin, X. Hou and J. Zhu, *ACS Applied Materials & Interfaces*, 2015, **7**, 696.

14 W. Zhao, J. Xu and H. Chen, *Chemical Society Reviews*, 2015, **44**, 729.

15 N.J. Ronkainen, H.B. Halsall and W.R. Heineman, *Chemical Society Reviews*, 2010, **39**, 1747.

16 F. Li, Y. Yu, H. Cui, D. Yang and Z. Bian, *Analyst*, 2013, **138**, 1844.

17 B. Lu, M.R. Smyth and R. O'Kennedy, *Analyst*, 1996, **121**, 29.

18 H. Wei and E. Wang, *Chemical Society Reviews*, 2013, **42**, 6060.

19 Y. Yan, Q. Liu, K. Wang, L. Jiang, X. Yang, J. Qian, X. Dong and B. Qiu, *Analyst*, 2013, **138**, 7101.

20 P. Si, Y. Huang, T. Wang and J. Ma, *Rsc Advances*, 2013, **3**, 3487.

21 J. Wang, *Microchimica Acta*, 2012, **177**, 245.

22 H. Zhang and N. Toshima, *Catalysis Science & Technology*, 2013, **3**, 268.

23 G. Fan, X. Ren, C. Zhu, J. Zhang and J. Zhu, *Biosensors and Bioelectronics*, 2014, **59**, 45.

24 J. Lei and H. Ju, *Chemical Society Reviews*, 2012, **41**, 2122.

25 J. Zeng, S. Fan, C. Zhao, Q. Wang, T. Zhou, X. Chen, Z. Yan, Y. Li, W. Xing and X. Wang, *Chemical Communications*, 2014, **50**, 8121.

26 Z. Gao, L. Hou, M. Xu and D. Tang, *Scientific Reports*, 2014, **4**, 1.

27 T.K. Sau and C.J. Murphy, *Langmuir*, 2004, **20**, 6414.

28 X. Zhou, X. Huang, X. Qi, S. Wu, C. Xue, F.Y.C. Boey, Q. Yan, P. Chen and H. Zhang, *The Journal of Physical Chemistry C*, 2009, **113**, 10842.

29 J. Li, X. Li, Y. Zhang, R. Li, D. Wu, B. Du, Y. Zhang, H. Ma and Q. Wei, *RSC Advances*, 2015, **5**, 5432.

30 N. Li, Y. Wang, Y. Li, W. Cao, H. Ma, D. Wu, B. Du and Q. Wei, *Sensors & Actuators B Chemical*, 2014, **202**, 67.

31 X. Ren, D. Wu, Y. Wang, Y. Zhang, D. Fan, X. Pang, Y. Li, B. Du and Q. Wei, *Biosensors and Bioelectronics*, 2015, **72**, 156.

32 X. Wei, C. Xiao, K. Wang and Y. Tu, *Journal of Electroanalytical Chemistry*, 2013, **702**, 37.

33 G. Jie, L. Wang, J. Yuan and S. Zhang, *Analytical Chemistry*, 2011, **83**, 3873.

34 Z. Zhang, Y. Wang, F. Zheng, R. Ren and S. Zhang, *Chemical Communications*, 2014, **51**, 907.

35 D. Wang and Y. Li, *Advanced Materials*, 2011, **23**, 1044.

36 C. Gao, M. Su, Y. Wang, S. Ge and J. Yu, *RSC Advances*, 2015, **5**, 28324.

37 X. Li, R. Wang and X. Zhang, *Microchimica Acta*, 2011, **172**, 285.

38 J. Ji, L. He, Y. Shen, P. Hu, X. Li, L. Jiang, J. Zhang, L. Li and J. Zhu, *Analytical Chemistry*, 2014, **86**, 3284.

39 D. Wang, Y. Li, Z. Lin, B. Qiu and L. Guo, *Analytical Chemistry*, 2015, **87**, 5966.

40 Z. Sun, L. Deng, H. Gan, R. Shen, M. Yang and Y. Zhang, *Biosensors and Bioelectronics*, 2013, **39**, 215.